Research Article

Dongsheng He, Beibei Chen, Yuan Tang*, Qianqian Li, Kecheng Zhang, Zhili Li, and Changming Xu

The enhanced adsorption properties of phosphorus from aqueous solutions using lanthanum modified synthetic zeolites

https://doi.org/10.1515/gps-2023-0106
received July 07, 2023; accepted October 09, 2023

Abstract: In this study, a modified synthetic zeolite adsorbent was synthesized by the hydrothermal method using coal fly ash as the main raw material, and the enhanced phosphorus adsorption properties from aqueous solutions were then evaluated. The modification parameters were specifically studied and optimized. Moreover, the effects of initial phosphorus concentration, adsorption time, and pH value on phosphorus absorption were also investigated. The adsorbent was characterized by the energy-dispersive spectrometer analysis, scanning electron microscopy, and Fourier transform infrared spectroscopy. Furthermore, the phosphorus adsorption properties of the zeolite adsorbent were preliminarily discussed through the perspectives of isothermal adsorption experiments, adsorption kinetics experiments, and adsorption thermodynamics calculations. The results show that the lanthanum ions were physically loaded on the surface and micropores of the adsorbent after modification, which helps to enhance the adsorption effect of phosphorus components from the aqueous solution. The phosphorus removal rate has been increased by about 65%. The adsorption process better fitted the Langmuir and Elovich equations. The theoretical calculation and analysis of adsorption thermodynamics showed that the adsorption and removal of phosphorus in water happens spontaneously.

Keywords: coal fly ash, lanthanum modification, phosphorus removal, adsorption properties

*** Corresponding author: Yuan Tang**, School of Resources and Safety Engineering, Wuhan Institute of Technology, Wuhan 430073, China, e-mail: yuan.tang@wit.edu.cn
Dongsheng He: School of Resources and Safety Engineering, Wuhan Institute of Technology, Wuhan 430073, China; Hubei Three Gorges Laboratory, Yichang 443007, China
Beibei Chen, **Qianqian Li**, **Zhili Li**, **Changming Xu:** School of Resources and Safety Engineering, Wuhan Institute of Technology, Wuhan 430073, China
Kecheng Zhang: School of Resources and Safety Engineering, Wuhan Institute of Technology, Wuhan 430073, China; Hubei Engineering Design & Research Institute Co. Ltd., Wuhan 430071, China

1 Introduction

The main chemical components in common phosphorus-containing wastewater are phosphates such as PO_4^{3-}, HPO_4^{2-}, and $H_2PO_4^-$ [1]. The large-scale discharge of phosphorus-containing wastewater will directly cause the eutrophication of water bodies and destroy its ecological balance [2]. At this stage, the removal methods of phosphorus components in water mainly include chemical precipitation, biological, adsorption, crystallization, and ion exchange methods [3]. Among them, the adsorption method has the advantages of easy operation, low cost, and no secondary pollution. It is regarded as one of the most potential methods of phosphorus removal in water [4,5]. The adsorption method mainly relies on the interaction between the adsorbent and phosphorus components in water (including physical or chemical adsorption) to achieve the purpose of phosphorus removal. It can be seen that the selection of high-efficiency adsorbents plays a key role in this process [6]. Research has found that the zeolite is a highly efficient absorbent, which has been widely used in water treatment because of its unique microstructures [7]. In addition, studies have pointed out that the chemical composition of coal fly ash contains a large proportion of SiO_2 and Al_2O_3, which is an ideal raw material for the synthesis of zeolite [8,9].

Coal fly ash is mainly a silver-gray or gray porous granular material produced by coal-fired thermal power plants, and is currently the largest industrial solid waste in China [10,11]. The national output of coal fly ash in 2020 has exceeded 650 million tons, in which the overall utilization rate of coal fly ash is only about 70% [12]. The accumulation of a large amount of coal fly ash will not only cause waste of land resources but also may cause water and soil pollution and destroy the ecological cycle if improperly handled. Therefore, it is of great practical significance to carry out

research on the utilization of coal fly ash [13]. Compared with other developed countries or regions, the utilization of coal fly ash in China mainly includes use as raw materials for the production of cement, building materials, and concrete [14,15], but the utilization in high value-added fields is still relatively low [16,17]. In recent years, the green and high-value utilization of coal fly ash has always been a hotspot in the research on industrial solid waste disposal, and it is also an urgent problem to be solved. Based on the observed phenomena reported earlier, the adsorption capacity of natural zeolite is better than that of coal fly ash, and the adsorption capacity of coal fly ash synthetic zeolite is the best of the three [3]. At present, many researchers have established a certain research basis for the treatment of phosphorus-containing wastewater using zeolite adsorbents synthesized from coal fly ash [18–22]. It is reported that the scheme has been proven to be effective in increasing the efficiency and saving the costs, without jeopardizing adsorption capacity. Furthermore, the modification treatments have been conducted to enhance the adsorption effect [23–26]. Some related researches indicate that the physicochemical properties and adsorption behavior of synthetic zeolites modified by rare earth were greatly enhanced [23,27–30]. However, a few studies focus on the phosphorus adsorption properties from aqueous solutions, such as the adsorption kinetics, adsorption thermodynamics, and adsorption isotherms.

In this study, the synthesized zeolite was modified by lanthanum chloride solution, which was used in the treatment of phosphorus-containing wastewater. Then, scanning electron microscopy coupled with energy-dispersive spectroscopy (SEM-EDS), Fourier transform infrared spectroscopy (FTIR), and other analysis and detection methods were applied for the characterization of the physicochemical properties of the synthesized zeolite before and after modification. For further investigation on the effect of lanthanum chloride modification on phosphorus adsorption properties from aqueous solutions, the perspectives of isothermal adsorption, adsorption kinetics, and adsorption thermodynamics of phosphorus components need to be determined. In short, it provides theoretical and experiment basis for the mechanism of rare earth element modification to strengthen the adsorption and phosphorus removal of coal fly ash synthetic zeolite.

2 Materials and methods

2.1 Materials

The coal fly ash used in the test was purchased from a coal-fired power plant in Hubei, China, which was fully mixed, ground, and dried at 105°C, and then passed through a 200-mesh standard sieve. The chemical composition of the samples was analyzed by using an X-ray fluorescence spectrometer (XRF, ARL PERFORM'X, Thermo Scientific, USA), and the results are presented in Table 1. As Table 1 shows, the main components are SiO_2 and Al_2O_3, which are consistent with the main components of natural zeolite.

The simulated phosphorus-containing aqueous solutions with different concentrations were prepared by diluting the 1,000 mg·L^{-1} potassium hydrogen phosphate stock solution. All the chemicals employed in this study were of analytical grade, and double distilled water was used throughout this study.

2.2 Preparation of zeolite adsorbents

2.2.1 Pretreatment of the coal fly ash

The coal fly ash and ultrapure water were mixed uniformly in a beaker at a solid-to-liquid ratio of 1 g:20 mL, and then the beaker was placed in a water-bath thermostatic magnetic stirrer at 25°C for 24 h. After water washing, the mixture was taken out and filtered with suction. Then, the washed coal fly ash was dried and sieved.

2.2.2 Synthesis of zeolite

Appropriate amounts of coal fly ash and 1 mol·L^{-1} NaOH solution were added into a round-bottomed flask at the solid-to-liquid ratio of 1 g:5 mL, and then evenly mixed. The suitable synthesis time, alkali concentration, and temperature for zeolite synthesis are 8 h, 1 mol·L^{-1}, and 120°C, respectively. After the synthetic experiment, the product was repeatedly washed with ultrapure water three times. Finally, the synthetic product was filtered, dried, and weighed.

2.2.3 Modification of the synthetic zeolite

The synthetic zeolite was added into a conical flask with 20 mL solution of the modifier. The mass concentrations of

Table 1: Results of elemental analysis of the coal fly ash samples (wt%)

Element	SiO_2	Al_2O_3	Fe_2O_3	CaO	MgO	K_2O	Others	Si/Al
Content	46.54	34.88	6.77	5.04	0.60	0.46	5.71	1. 18

the lanthanum chloride modifier were chosen in the range of 0.4–2.0%. The pH value of the pulp was adjusted with sodium hydroxide (NaOH) and hydrochloric acid (HCl) (Sinopharm Chemical Reagent Co., Ltd, Shanghai, China). Then, the influence of the solid–liquid ratio on the modification was studied to explore the optimum modification conditions. After the modification, the synthetic zeolite was repeatedly washed with ultrapure water for three times. Finally, the effects of modification on phosphorus removal were determined through adsorption experiments.

2.3 Physicochemical properties of zeolite adsorbents

2.3.1 SEM analysis

Microstructures for the zeolite adsorbents were studied by SEM (JSM-5510LV, JEOL, Japan). In each experiment, the pressure, accelerated voltage, and work distance were set to 30 Pa, 15 kV, and 10–12 mm, respectively.

2.3.2 FTIR spectroscopy measurements

FTIR spectroscopy has been widely used to identify the adsorption approach of the reagents on solid surfaces. One gram of the ground zeolite adsorbent (<5 μm) was mixed with the spectroscopic KBr and determined within the wavenumber range of 4,000–400 cm^{-1} at a resolution of 2 cm^{-1}. The infrared spectra were determined with an FTIR spectrometer (Continuum XL, Thermo Scientific, USA).

2.3.3 EDS analysis

Chemical composition of the synthetic zeolite and its modified products was analyzed by using the FALCON8200 EDAX instrument (AMETEK, USA). The EDS examination was performed using a beam current and a beam size of 1 nA and 1 μm, respectively. In each quantification, a dwell time of 30 s was applied.

2.4 Adsorption tests

A certain amount of modified zeolite adsorbent was added into a 50 mL centrifuge tube together with 40 mL of simulated phosphorus-containing wastewater (initial concentrations were controlled to be 10–500 $mg{\cdot}L^{-1}$), and the adsorption tests were conducted to evaluate the phosphorus removal effect. In these cases, the pH value was adjusted between 2 and 12. After adsorption, the remaining total phosphorus in the supernatant was measured by ammonium molybdate spectrophotometry [31], and the phosphorus removal rate was relatively calculated. The total phosphorus concentration (C_p), phosphorus removal rate (R), and adsorption amount (Q) in the solution can be described by Eqs. 1, 2, and 3, respectively.

$$C_p = \frac{A_s - A_b - b}{a} \tag{1}$$

$$R = \frac{C_0 - C_e}{C_0} \times 100\% \tag{2}$$

$$Q = \frac{(C_0 - C_e) \times V}{m \times 1{,}000} \tag{3}$$

where C_p is the concentration of total phosphorus (calculated by element) in the solution ($mg{\cdot}L^{-1}$), A_s is the absorbance of the solution, A_b is the absorbance of the blank test, a is the slope of the calibration curve, b is the intercept of the calibration curve, R is the removal rate of phosphorus (%), Q is the adsorption amount of phosphorus ($mg{\cdot}g^{-1}$), C_0 is the initial concentration of phosphorus ($mg{\cdot}L^{-1}$), C_e is the equilibrium concentration of phosphorus ($mg{\cdot}L^{-1}$), V is the solution volume (mL), and m is the mass of zeolite (g).

2.5 Specific surface area analysis

The BET-specific surface area and average pore volume of the prepared adsorbent before and after phosphorus adsorption were analyzed by using a Autosorb-iQ instrument (Quantachrome, USA). Each measurement was conducted three times, and the average result was recorded.

3 Results and discussion

3.1 Influencing factors of zeolite modification

3.1.1 Effect of modifier concentration

Figure 1(a) shows the influence of lanthanum concentration on the phosphorus removal of synthesized zeolite from coal fly ash. With the increase of lanthanum concentration, the

phosphorus removal rate and the adsorption amounts increase gradually. When the lanthanum concentration was 1.2%, the phosphorus removal rate and the adsorption amounts reached the maximum at 98.6% and 1.97 mg·g^{-1}, respectively. After that, the removal rate began to decrease slowly, and the corresponding adsorption capacities also decreased. It might be that as the concentration of lanthanum ions increases, the coordination complexes formed between lanthanum ions and synthetic zeolite components transform from adsorbing phosphate at the initial stage to blocking the pores of synthetic zeolite, resulting in a decrease in the phosphorus removal [32,33]. According to the test data, 1.2% lanthanum chloride solution was determined as a reasonable modification concentration in the subsequent modification test.

3.1.2 Effect of pH

Figure 1(b) shows that the pH has a great influence on the phosphorus removal of synthesized zeolite from coal fly ash. When the pH value of the modified solution was lower than 5, the removal rate and adsorption capacities of the synthetic zeolite increased with the increase in the pH value. While the pH increased from 5 to 7, the phosphorus removal rate and adsorption capacity decreased slightly. Furthermore, the removal rate and adsorption capacities increase monotonically with the increase in pH from 7 to 12. At pH 10, the removal rate of phosphorus reached 95.8%, and the corresponding adsorption amount reached 1.91 mg·g^{-1}. The appropriate pH of the modified solution was determined to be 10, which is also consistent with the results reported in the study by Wang [34].

3.1.3 Effect of solid–liquid ratio

The effect of the solid-to-liquid ratio (the ratio of the mass of synthesized zeolite to the volume of lanthanum chloride solution, g·mL^{-1}) on the phosphorus removal performance of zeolite synthesis from coal fly ash is presented in Figure 1(c). When the solid–liquid ratio was 1 g:3 mL, the phosphorus removal rate and adsorption capacities of the modified zeolite are only 31.7% and 0.63 mg·g^{-1}, respectively.

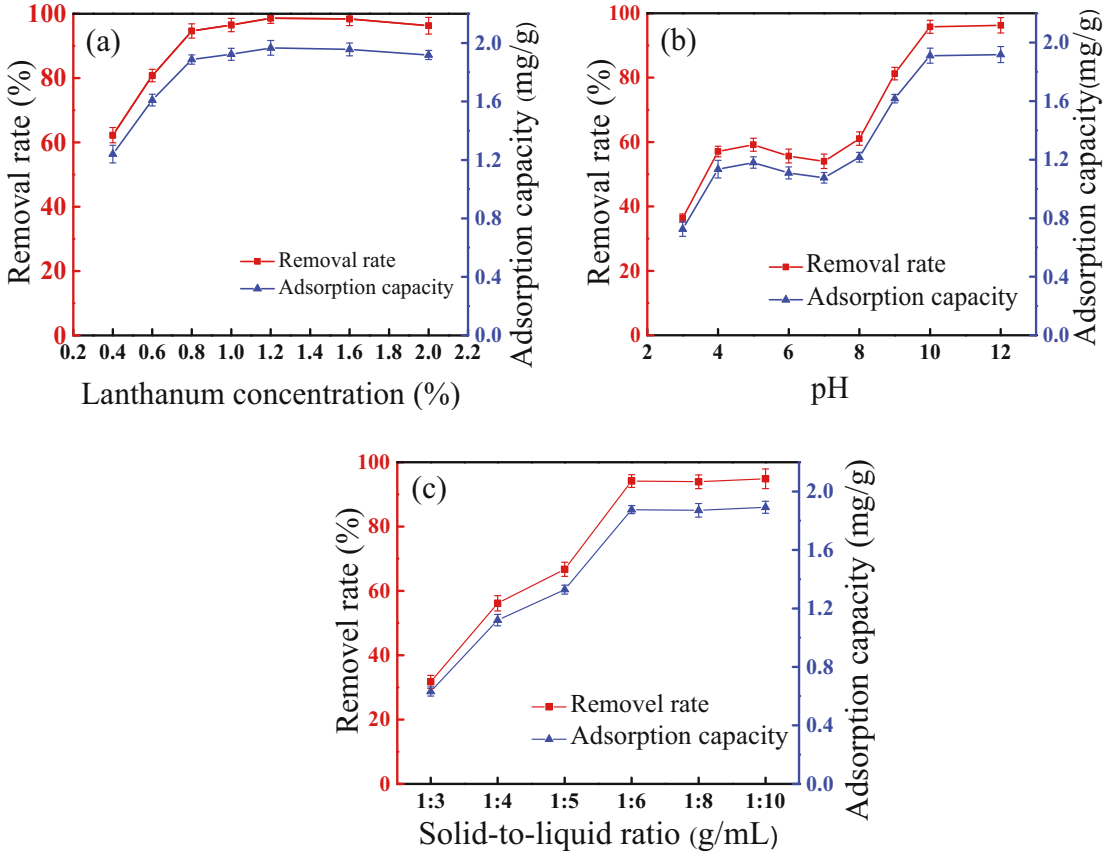

Figure 1: Phosphorus removal ability under different (a) lanthanum concentrations, (b) pH values, and (c) solid-to-liquid ratios.

While the solid-to-liquid ratio becomes smaller, the removal rate of phosphorus in water by the modified zeolite increases continuously. When the solid–liquid ratio is 1 g:6 mL, the phosphorus removal rate reached 94.2%. If the solid-to-liquid ratio continues to decrease, the phosphorus removal rate does not change much. The more lanthanum ions there is, the more active adsorbents are loaded into the synthetic zeolite, and these substances have good adsorption to phosphate, so the removal effect of modified zeolite on phosphorus in the solution showed a trend of first increasing significantly and then reaching a stable level. According to the test results, the economic efficiency of the modification of synthetic zeolite and the high efficiency of phosphorus removal are combined to determine the suitable concentration of lanthanum chloride solution, pH of the modified solution, and solid-to-liquid ratio for the optimization and modification of lanthanum chloride modified coal fly ash zeolite as 1.2%, 10, and 1 g:6 mL, respectively.

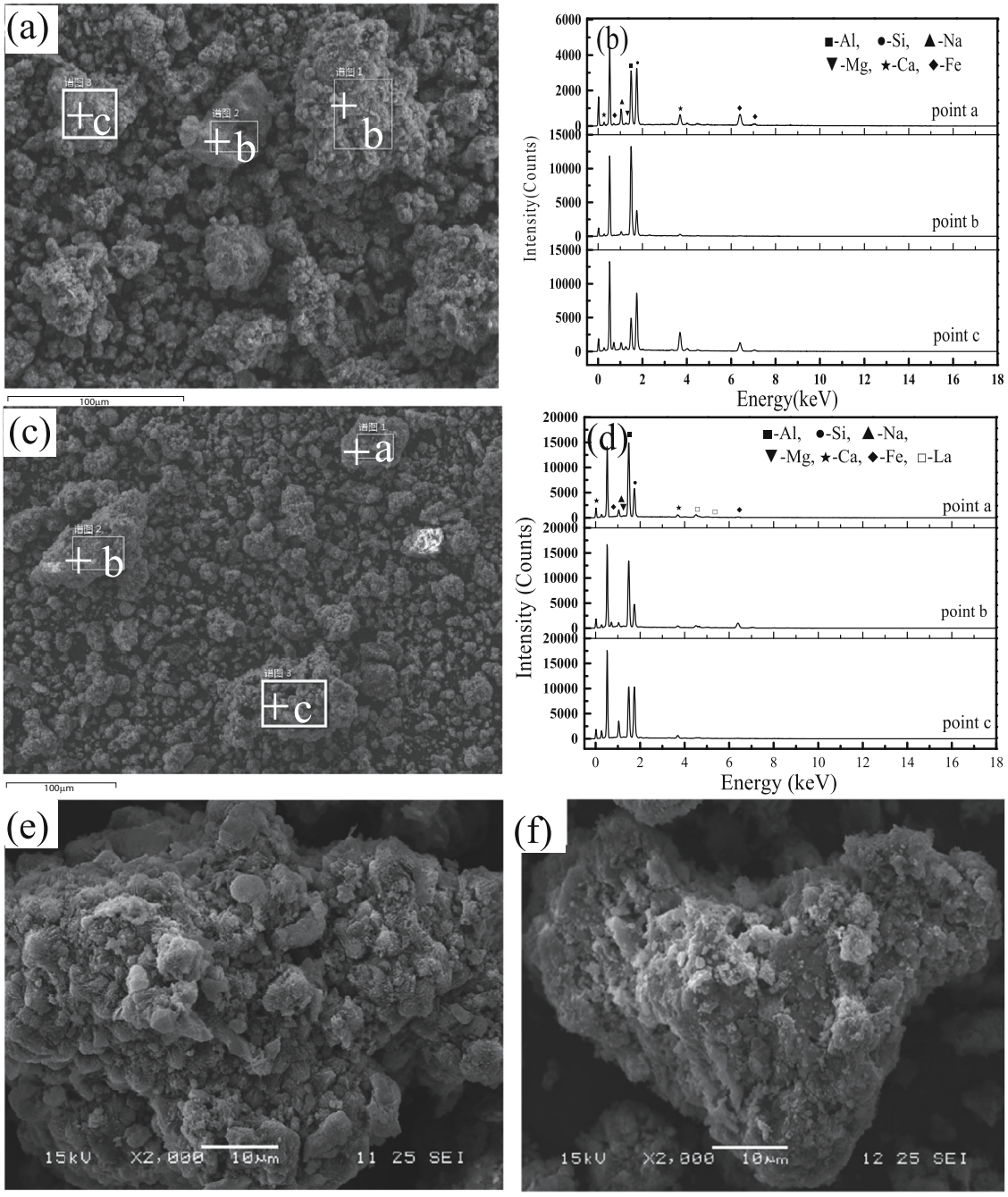

Figure 2: SEM and EDS analyses of the synthetic zeolite (a, b, and e) before and (c, d, and f) after modification.

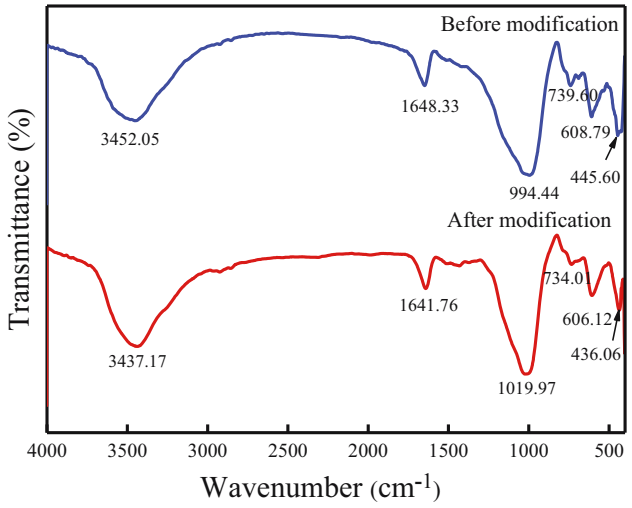

Figure 3: FTIR characterization of the synthetic zeolite before and after modification.

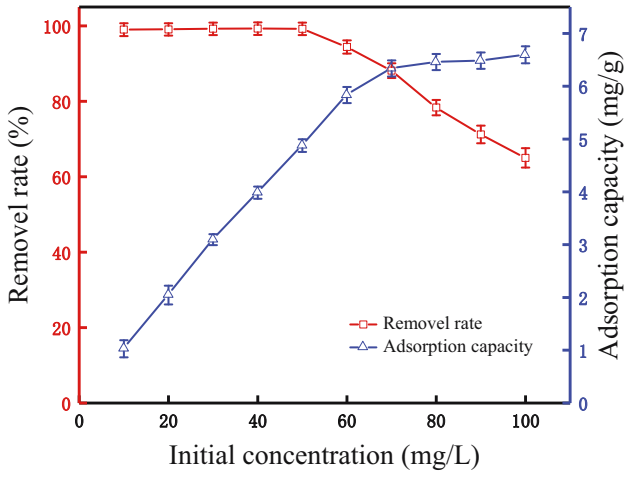

Figure 4: Effect of initial phosphorus concentration on phosphorus removal.

3.2 Physicochemical properties

3.2.1 SEM and EDS analysis

SEM and EDS analyses of the synthetic zeolite adsorbent were made so as to ascertain its chemical composition and microscopic structure before and after modification with lanthanum chloride. It can be seen that the main chemical components of the synthetic zeolite (Figure 2(b)) and the modified synthetic zeolite (Figure 2(d)) are silicon, aluminum, iron, calcium, magnesium, and so on. It might be possible to deduce that the content of lanthanum ions in the synthetic zeolite was significantly increased, which indicated that lanthanum ions have been successfully

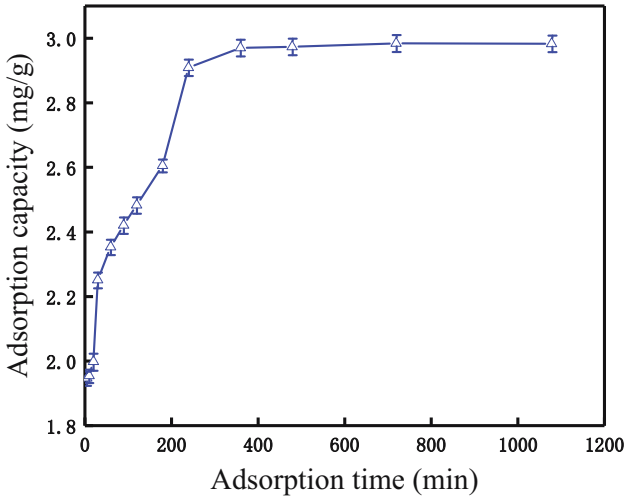

Figure 5: Effect of adsorption time on phosphorus removal.

introduced into the synthesized zeolite, so that the phosphorus removal capacity has been significantly improved. SEM images (in Figure 2(e) and (f)) have also been taken to show the particle morphology of the synthetic zeolite adsorbent before and after modification. The results showed that the morphology was changed to a certain extent when the synthetic zeolite was modified with lanthanum chloride. The surface of the unmodified synthetic zeolite was rough and has many protrusions, which generally showed the typical morphology of P-type zeolite particles, while the surface of the modified synthetic zeolite was relatively smooth and fuzzy. On the whole, the result shown in Figure 2 shows that lanthanum was introduced onto the synthetic zeolite surface after the modification, but does not change the structure.

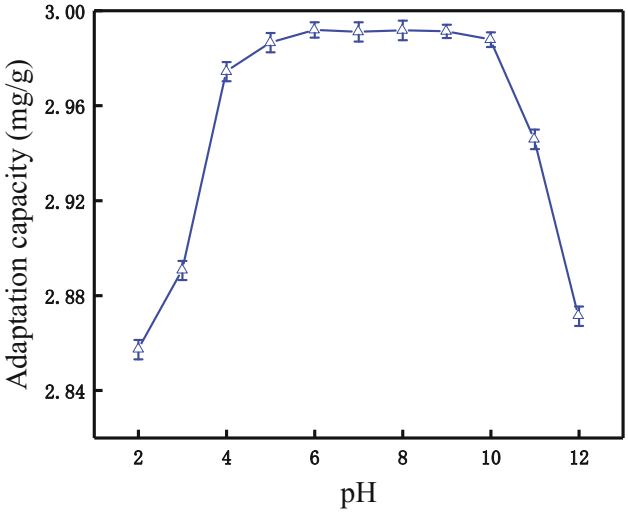

Figure 6: Effect of pH on phosphorus removal.

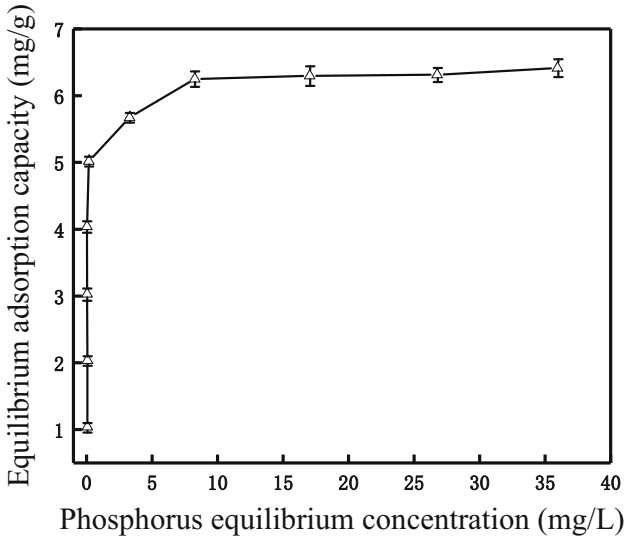

Figure 7: Adsorption isotherm of phosphorus by the modified synthetic zeolites.

3.2.2 FTIR characterization

Figure 3 shows the infrared absorption spectrum of the synthetic zeolite treated with or without the lanthanum chloride solution. It indicates that the infrared absorption peaks of the synthetic zeolite from coal fly ash at 445.60 and 608.79 cm^{-1} might be caused by the bending vibration of Si–O or the double ring vibration of O–Si(Al)–O [35]. The peak appeared at 739.60 cm^{-1} means the stretching vibration of the tetrahedral structure, and the strong absorption peak at 994.44 cm^{-1} is the asymmetric stretching vibration of the Si(Al)–O–Si. The peaks of 1,648.33 and 3,452.05 cm^{-1} are the bending and stretching vibrations of the hydroxyl groups of water molecules adsorbed by zeolite, respectively, which are consistent with related studies [36,37].

3.3 Influencing factors of phosphorus adsorption

3.3.1 Effect of phosphorus initial concentration

Figure 4 shows the effect of phosphorus initial concentration on the phosphorus removal effect of the modified synthetic zeolites in water. When the initial concentration of phosphorus was at 10–70 $mg{\cdot}L^{-1}$, the adsorption capacity of the modified synthetic zeolites to phosphorus increased rapidly with the increase of the initial concentration of simulated wastewater. It indicates that the active sites of the modified synthetic zeolites within this concentration range were sufficient to remove phosphorus in water [38]. Furthermore, the adsorption capacity of the modified synthetic zeolites might suffer due to the reduction of active sites on the surface when the initial concentration was more than 70 $mg{\cdot}L^{-1}$.

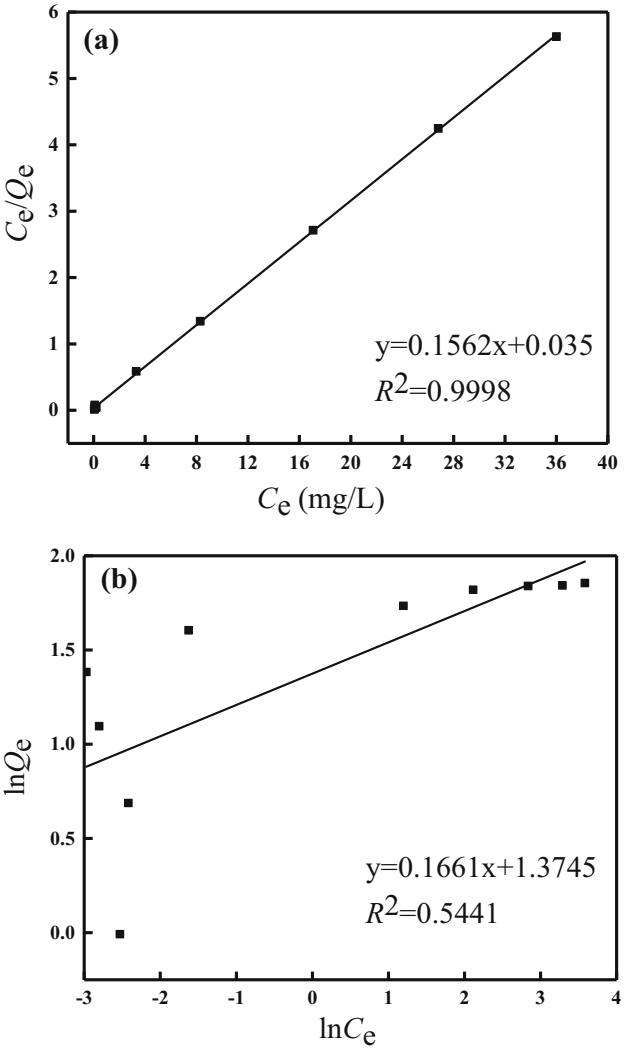

Figure 8: Linear fitting of (a) Langmuir and (b) Freundlichadsorption isotherm model.

Table 2: Linear fitting parameters of the two isothermal adsorption models

Models	Langmuir adsorption isotherm model			Freundlich adsorption isotherm model		
	Q_m ($mg{\cdot}g^{-1}$)	K_L ($L{\cdot}mg^{-1}$)	R^2	K_F	1/n	R^2
Values	6.40	4.463	0.9998	3.953	0.166	0.5441

3.3.2 Effect of adsorption time

As shown in Figure 5, the adsorption process of the modified synthetic zeolites conforms to the characteristics of "rapid adsorption in the early stage and slow equilibrium in the later stage" [39], that is, when the adsorption time was less than 300 min, the phosphorus adsorption increases rapidly, and then the adsorption capacity gradually becomes flat and basically unchanged after 400 min. The removal rate of phosphorus reaches the maximum of 96.9% at 360 minutes, and the corresponding adsorption capacity increased to 2.98 mg·g^{-1}.

3.3.3 Effect of pH

The solution pH has a great influence on the adsorption process [40]. Figure 6 shows the adsorption capacity of the modified synthetic zeolites as a function of pH value. It indicates that the adsorption capacity was low at a pH of less than 3.0. At pH 3.0–8.0, the phosphorus adsorption capacity gradually increases with the increase of pH, and the adsorption capacity increased from 2.89 to 2.99 mg·g^{-1}. Instead, at pH over 8.0, the phosphorus adsorption capacity decreases gradually. The adsorption capacity under strong acid conditions was likely to be related to the changes in pore structures of the synthetic zeolites, which makes zeolite unable to adsorb and fix phosphate.

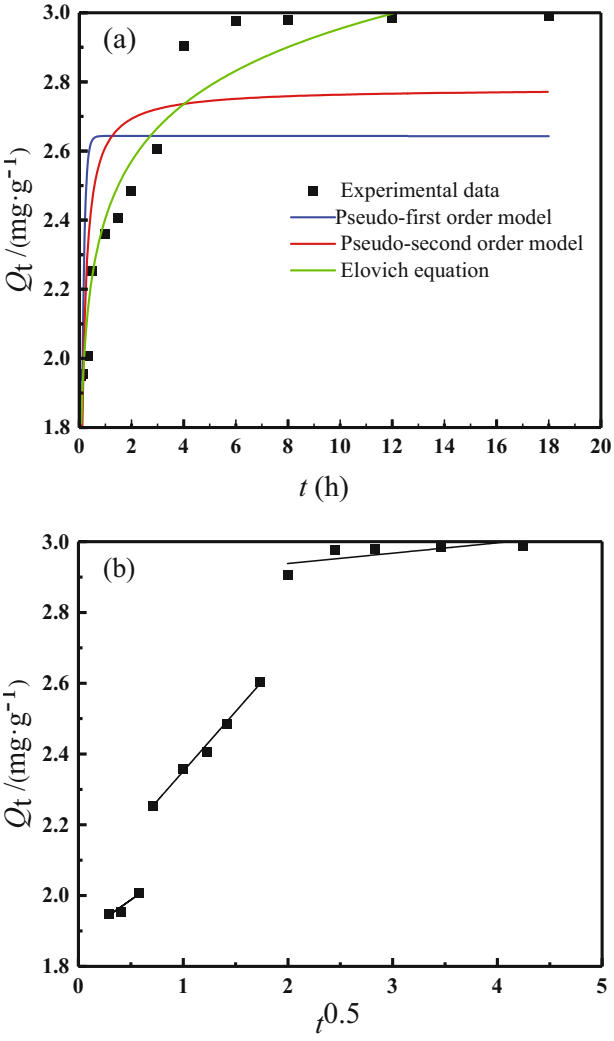

Figure 9: (a) Adsorption kinetic fitting results and (b) three-stage fitting curve of intraparticle diffusion model.

3.4 Phosphorus adsorption isotherms

The adsorption isotherm results of the modified synthetic zeolites are shown in Figure 7. It indicated that with the increase of phosphorus equilibrium concentration, the equilibrium adsorption capacity gradually increased. Moreover, Langmuir and Freundlich adsorption isotherm models were commonly used adsorption isotherm models, which belong to chemical adsorption and physical adsorption models, respectively [9]. In this study, the two models were used to describe the phosphorus adsorption behaviors. The linear forms of the Langmuir and Freundlich isotherm models are described by Eqs. 4 and 5, respectively [41].

$$\frac{C_e}{Q_e} = \frac{C_e}{Q_m} + \frac{1}{K_L Q_m} \tag{4}$$

$$\ln Q_e = \ln K_F + \frac{1}{n} \ln C_e \tag{5}$$

where C_e is the equilibrium mass concentration of pollutants in the solution (mg·L^{-1}), Q_e is the equilibrium adsorption capacity of the material to the pollutant (mg·g^{-1}), Q_m is the saturated adsorption capacity of the material to the pollutant (mg·g^{-1}), K_L and K_F are Langmuir and Freundlich equilibrium constants, respectively, and n is the Freundlich adsorption index.

According to the results shown in Figure 7, the Langmuir and Freundlich isotherm adsorption models were used for linear fitting, and the results are shown in Figure 8(a) and (b), respectively. The parameters of the adsorption isotherm models after linear fitting are shown in Table 2. It can be seen from the fitting results that the regression coefficients R^2 of the two models are 0.9998 and 0.5441, respectively, indicating that the Langmuir model is more suitable to describe the isothermal adsorption behavior and the adsorption process fitted the monolayer adsorption. The theoretical saturated adsorption capacity of modified zeolite for phosphorus in water calculated according to

Table 3: Fitting parameters of adsorption kinetic model

Model parameters	Pseudo-first-order kinetic model			Pseudo-second-order kinetic model			Elovich equation		
	Q_e (mg·g^{-1})	k_1 (h^{-1})	R^2	Q_e (mg·g^{-1})	k_2 (g·mg^{-1}·h^{-1})	R^2	a (g·mg^{-1}·h^{-1})	b (g·mg^{-1})	R^2
Parameter value	2.64	10.786	0.3299	2.78	5.469	0.6513	5,561.92	4.185	0.9375

the Langmuir model was 6.4 mg·g^{-1}, which was very close to the actual saturated adsorption capacity (6.3 mg·g^{-1}). The calculated separation constant R_L of the modified synthetic zeolites was between 0 and 1, indicating that the phosphorus could be effectively adsorbed in water. The fitting constant $1/n$ was in the range of 0–0.5, indicating that the phosphorus adsorption process was easy to carry out.

3.5 Phosphorus adsorption kinetics

In general, the phosphate adsorption process of the modified synthetic zeolites can also be seen as a process of internal diffusion and adsorption [8]. For better understanding and evaluating the adsorption process, four models of pseudo-first-order, pseudo-second-order, intraparticle diffusion model, and Elovich equation model [42–44] (Eqs. 6–9) were used to study the adsorption kinetics.

Pseudo-first-order model:

$$\ln(Q_e - Q_t) = \ln Q_e - k_1 t \tag{6}$$

Pseudo-second-order model:

$$\frac{t}{Q_t} = \frac{t}{Q_e} + \frac{1}{k_2 Q_e^2} \tag{7}$$

Intraparticle diffusion model:

$$Q_t = k_d t^{0.5} + C \tag{8}$$

Elovich equation model:

$$Q_t = \frac{1}{b}\ln(a \times b \times t + 1) \tag{9}$$

Here, Q_t is the adsorption capacity at t (mg·g^{-1}); Q_e is the equilibrium adsorption capacity (mg·g^{-1}); k_1, k_2, and k_d represent the rate constant; t is the reaction time (h); C is the thickness of the adsorbent boundary layer; a is the initial adsorption rate (g·mg^{-1}·h^{-1}); and b is the analytical constant (g·mg^{-1}).

The fitting curves and correlation coefficients are shown in Figure 9 and Table 3, respectively. Results show that the Elovich equation model fitted the best, being 0.9375 in regression coefficient R^2, higher than the other two (Figure 9(a)). The pseudo-first-order kinetic model was the worst fitting, which shows that the phosphorus adsorption belongs to the chemical adsorption process of uneven solid surface, and it also shows that the surface adsorption energy of modified zeolite is evenly distributed in the whole adsorption process [45]. In Figure 9(b), the intraparticle diffusion process was divided into three stages, and the calculated fitting parameters for each stage are shown in Table 4. The fitting results show that the fitting correlation coefficient of the modified synthetic zeolites in the second stage is 0.9924, which indicated that the adsorption reaction of phosphorus on the surface of the modified synthetic zeolites is probably more up the intraparticle diffusion kinetic model. From Figure 9(b), the linearly fitted straight line did not pass through the origin over the entire time range, indicating that the intraparticle diffusion model was not the only rate-limiting mechanism and that there were other kinetic models controlling the adsorption rate [46].

3.6 Phosphorus adsorption thermodynamics

The thermodynamic parameters are often used to explore the change of heat in the phosphorus removal, so as to further explore the state characteristics of the modified synthetic zeolites [31]. K_e and the thermodynamic constants of ΔH^0 and ΔS^0 conform to the Van't Hoff equation [47] in the normal form (Eq. 10):

Table 4: Three-stage fitting parameters of the modified synthetic zeolites intraparticle diffusion model

Model parameters	Stage one			Stage two			Stage three		
	k_{d1} (mg·g^{-1}·h$^{-0.5}$)	C_1	R^2	k_{d2} (mg·g^{-1}·h$^{-0.5}$)	C_2	R^2	k_{d3} (mg·g^{-1}·h$^{-0.5}$)	C_3	R^2
Parameter value	0.209	1.88	0.8881	0.337	2.01	0.9924	0.029	2.88	0.5357

Table 5: Thermodynamic parameters of the modified synthetic zeolites in the phosphorus adsorption

ΔH^0 (kJ·mol^{-1})	ΔS^0 (J·mol^{-1}·K^{-1})	R^2	$\Delta G°$ (kJ·mol^{-1})				
			288 K	293 K	298 K	303 K	308 K
41.719	164.13	0.9854	−5.550	−6.371	−7.192	−8.012	−8.833

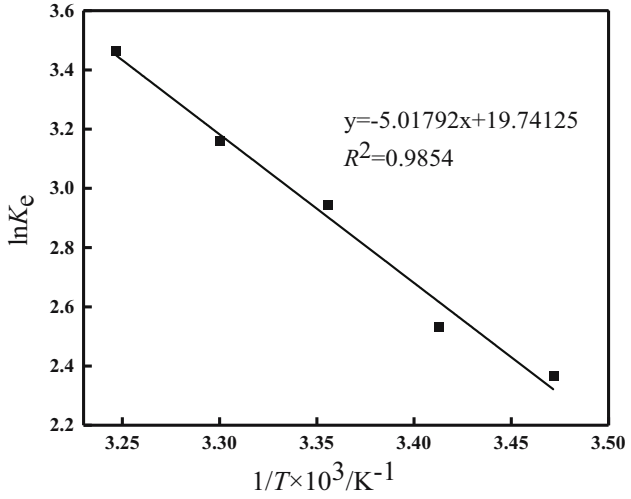

Figure 10: Relationship between ln K_e and 1/T of phosphorus removal by the modified synthetic zeolites.

Table 6: Results of specific surface area measurement

Adsorption state	BET-specific surface area (m^2·g^{-1})	Average pore volume (cm^3·g^{-1})
Before adsorption	42.074	0.238
After adsorption	40.125	0.201

$$\ln K_e = \frac{\Delta S^0}{R} - \frac{\Delta H^0}{RT} \quad (10)$$

where R is the ideal gas constant (8.314 J·(mol^{-1}·K^{-1}), T is the absolute temperature (K), and K_e is the equilibrium adsorption partition coefficient (mL·g^{-1}).

The adsorption thermodynamics is mainly carried out by studying the thermodynamic parameters, which are calculated as shown in Table 5. The fitting results are presented in Figure 10. Results show that the value of $\Delta G°$ was negative at different temperatures, indicating that the adsorption process can proceed spontaneously at all temperatures. As the temperature increases, $\Delta G°$ gradually decreases, which indicates that the higher the temperature, the greater the degree of spontaneity. Moreover, the whole process of ΔH^0 was positive, so it can be shown that the adsorption of phosphorus onto the modified synthetic zeolites was an endothermic reaction. Besides this, the value of ΔS^0 was positive indicating an increase in solid–liquid interfacial disorder and a decrease in orderliness during phosphorus adsorption by modified synthetic zeolites [47].

3.7 BET-specific surface area determination

As illustrated in Table 6, the specific surface area of the prepared adsorbent after phosphorus adsorption becomes smaller than that in the absence of phosphorus-containing solution, indicating that the introduction of prepared adsorbent in solution leads to alteration of surface morphology, which can apparently result from the reaction of phosphorus components with adsorbent. Furthermore, the average pore volume was decreased from 0.238 to 0.201 cm^3·g^{-1} showing that the phosphorus could be adsorbed into the microporous structure of the adsorbent.

4 Conclusion

In this study, the lanthanum concentration, pH, and solid-to-liquid ratio make an important influence on the modification of the synthetic zeolites. The modified synthetic zeolites were then characterized and verified the adsorption capacities for phosphorus. The results of SEM, EDS, and FTIR indicated that after the modification of lanthanum chloride, lanthanum was only loaded on the surface and micropores of zeolite synthesized, and did not change its crystal structure and skeleton structure, nor participate in skeleton vibration. The modified synthetic zeolites prepared at the conditions of modifier concentration of 1.2%, pH value of modified solution of 10, and solid–liquid ratio of 1 g: 6 mL showed the best adsorption capacities. The phosphorus adsorption of the modified synthetic zeolites belongs to the single molecular layer adsorption, and the adsorption isotherm was more in line with the Langmuir model. The adsorption kinetics analysis shows that the adsorption conforms to the Elovich equation. Thermodynamic studies have shown that the adsorption of phosphorus on modified zeolite belonged to the spontaneous process of endothermic

entropy increase. Furthermore, the reuse of zeolite adsorbent in phosphorus removal will be observed and discussed in a subsequent article.

Acknowledgments: We applied the SDC approach for the sequence of authors.

Funding information: This work was financially supported by the National Natural Science Foundation of China (grant number 52104263), the Key Research and Development Program of Hubei Province of China (grant number 2023BCB079), the National Key Research and Development Program of China (grant number 2022YFC2904701), and the Scientific Research Foundation of Wuhan Institute of Technology (grant number K2021099).

Conflict of interest: The authors state no conflict of interest.

Data availability statement: The datasets generated during and/or analyzed during the current study are available from the corresponding author on reasonable request.

References

[1] Dalu T, Wasserman RJ, Magoro ML, Froneman PW, Weyl OL. River nutrient water and sediment measurements inform on nutrient retention, with implications for eutrophication. Sci Total Environ. 2019;684:296–302. doi: 10.1016/j.scitotenv.2019.05.167.

[2] Huang W, Jin ZH, Yang HR, Qu YH, Che FF, Xu ZS, et al. Interception of phosphorus release from sediment by magnetite/lanthanum carbonate co modified activated attapulgite composite: Performance and mechanism. Colloids Surf, A. 2023;664:131139. doi: 10.1016/j.colsurfa.2023.131139.

[3] Ramasahayam SK, Guzman L, Gunawan G, Viswanathan T. A comprehensive review of phosphorus removal technologies and processes . J Macromol Sci, Part A. 2014;51(6):538–45. doi: 10.1080/10601325.2014.906271.

[4] Han MY, Shen XY, Shao HM, Liu Y, Han Q, Zhai YC. Facile one-pot hydrothermal synthesis of reticulated porous tobermorite for fast phosphorus recovery. Colloids Surf, A. 2023;666:131349. doi: 10.1016/j.colsurfa.2023.131349.

[5] dos Reis GS, Thue PS, Cazacliu BG, Lima EC, Sampaio CH, Quattrone M, et al. Effect of concrete carbonation on phosphate removal through adsorption process and its potential application as fertilizer. J Cleaner Prod. 2020;256:120416. doi: 10.1016/j.jclepro.2020.120416.

[6] Hussain Z, Chang N, Sun JQ, Xiang S, Ayaz T, Zhang H, et al. Modification of coal fly ash and its use as low-cost adsorbent for the removal of directive, acid and reactive dyes. J Hazard Mater. 2022;422:126778. doi: 10.1016/j.jhazmat.2021.126778.

[7] Murakami T, Otsuka K, Fukasawa T, Ishigami T, Fukui K. Hierarchical porous zeolite synthesis from coal fly ash via microwave heating. Colloids Surf, A. 2023;661:130941. doi: 10.1016/j.colsurfa.2023.130941.

[8] Wen ZP, Chen HC, Pan JH, Jia RB, Yang F, Liu HT, et al. Grinding activation effect on the flotation recovery of unburned carbon and leachability of rare earth elements in coal fly ash. Powder Technol. 2022;398:117045. doi: 10.1016/j.powtec.2021.117045.

[9] He XP, Yao B, Xia Y, Huang H, Gan YP, Zhang WK. Coal fly ash derived zeolite for highly efficient removal of Ni2+ inwaste water. Powder Technol. 2020;367:40–6. doi: 10.1016/j.powtec.2019.11.037.

[10] Hussain Z, Lizhen G, Moeen M. Treatment of coal fly ash and environmentally friendly use with rubber in cable wires as insulation material. Sustainability. 2020;12(12):5218. doi: 10.3390/su12125218.

[11] Wang ZH, Xu LH, Wu DS, Zheng SL. Hydrothermal synthesis of mesoporous tobermorite from fly ash with enhanced removal performance towards Pb2+ from wastewater. Colloids Surf, A. 2022;632:127775. doi: 10.1016/j.colsurfa.2021.127775.

[12] Luo Y, Wu Y, Ma S, Zheng S, Zhang Y, Chu PK. Utilization of coal fly ash in China: a mini-review on challenges and future directions. Environ Sci Pollut Res. 2021;28:18727–40. doi: 10.1007/s11356-020-08864-4.

[13] Mushtaq F, Zahid M, Bhatti IA, Nasir S, Hussain T. Possible applications of coal fly ash in wastewater treatment. J Environ Manage. 2019;240:27–46. doi: 10.1016/j.jenvman.2019.03.054.

[14] Yao ZT, Ji XS, Sarker PK, Tang JH, Ge LQ, Xia MS, et al. A comprehensive review on the applications of coal fly ash. Earth-Sci Rev. 2015;141:105–21. doi: 10.1016/j.earscirev.2014.11.016.

[15] Gollakota ARK, Volli V, Shu CM. Progressive utilization prospects of coal fly ash: A review. Sci Total Environ. 2019;672:951–89. doi: 10.1016/j.scitotenv.2019.03.337.

[16] Xing YW, Guo FY, Xu MD, Gui XH, Li HS, Li GS, et al. Separation of unburned carbon from coal fly ash: A review. Powder Technol. 2019;353:372–84. doi: 10.1016/j.powtec.2019.05.037.

[17] Wang NN, Zhao Q, Li QY, Zhang GS, Huang YL. Degradation of polyacrylamide in an ultrasonic-Fenton-like process using an acid-modified coal fly ash catalyst. Powder Technol. 2020;369:270–8. doi: 10.1016/j.powtec.2020.05.052.

[18] Kobayashi Y, Ogata F, Nakamura T, Kawasaki N. Synthesis of novel zeolites produced from fly ash by hydrothermal treatment in alkaline solution and its evaluation as an adsorbent for heavy metal removal. J Environ Chem Eng. 2020;8(2):103687. doi: 10.1016/j.jece.2020.103687.

[19] Estevam ST, de Aquino TF, da Silva TD, da Cruz R, Bonetti B, Riella HG, et al. Synthesis of K-Merlinoite zeolite from coal fly ash for fertilizer application. Braz J Chem Eng. 2021;39:631–43. doi: 10.1007/s43153-021-00172-9.

[20] Koshy N, Singh DN. Fly ash zeolites for water treatment applications. J Environ Chem Eng. 2016;4(2):1460–72. doi: 10.1016/j.jece.2016.02.002.

[21] Zhang KC, Van Dyk L, He DS, Deng J, Liu S, Zhao HQ. Synthesis of zeolite from fly ash and its adsorption of phosphorus in wastewater. Green Process Synth. 2021;10(1):349–60. doi: 10.1515/gps-2021-0032.

[22] Molina A, Poole C. A comparative study using two methods to produce zeolites from fly ash. Miner Eng. 2004;17(2):167–73. doi: 10.1016/j.mineng.2003.10.025.

[23] Goscianska J, Ptaszkowska-Koniarz M, Frankowski M, Franus M, Panek R, Franus. W. Removal of phosphate from water by lanthanum-modified zeolites obtained from fly ash. J Colloid Sci. 2018;513:72–81. doi: 10.1016/j.jcis.2017.11.003.

[24] Shukla EA, Johan E, Henmi T, Matsue N. Arsenate adsorption on iron modified artificial zeolite made from coal fly ash. Procedia Environ Sci. 2013;17:279–84. doi: 10.1016/j.proenv.2013.02.039.
[25] Nascimento M, Soares PSM, de Souza VP. Adsorption of heavy metal cations using coal fly ash modified by hydrothermal method. Fuel. 2009;88(9):1714–9. doi: 10.1016/j.fuel.2009.01.007.
[26] Qiu QL, Jiang XG, Lv GJ, Chen ZL, Lu SY, Ni MJ, et al. Adsorption of heavy metal ions using zeolite materials of municipal solid waste incineration fly ash modified by microwave-assisted hydrothermal treatment. Powder Technol. 2018;335:156–63. doi: 10.1016/j.powtec.2018.05.003.
[27] Asaoka S, Kawakami K, Saito H, Ichinari T, Nohara H, Oikawa T. Adsorption of phosphate onto lanthanum-doped coal fly ash—Blast furnace cement composite. J Hazard Mater. 2021;406:124780. doi: 10.1016/j.jhazmat.2020.124780.
[28] Xu R, Lyu T, Wang LJ, Yuan YT, Zhang MY, Cooper M, et al. Utilization of coal fly ash waste for effective recapture of phosphorus from waters. Chemosphere. 2022;287:132431. doi: 10.1016/j.chemosphere.2021.132431.
[29] Wang W, Qi L, Zhang P, Luo J, Li J. Removal of COD in wastewater by magnetic coagulant prepared from modified fly ash. Environ Sci Pollut Res. 2022;29(34):52175–88. doi: 10.1007/s11356-022-19540-0.
[30] Zhang L, Qin Y, Zhang X, Gao X, Song L. Further findings on the stabilization mechanism among modified Y zeolite with different rare earth ions. Ind Eng Chem Res. 2019;58(31):14016–25. doi: 10.1021/acs.iecr.9b03036.
[31] Yang CX, Sun XY, Liu B, Lian HT. Determination of total phosphorus in water sample by digital imaging colorimetry. Chin J Anal Chem. 2007;35(6):850–3. doi: 10.1016/S1872-2040(07)60059-0.
[32] Wang YU, Chen JN, Li XM, Luo Q, Yang Q, Jiang. L. Stimultaneous removal of ammonium and phosphate in waste water by La-modified synthetic zeolite from coal fly ash. China Environ Sci. 2011;31(7):1152–8. doi: 10.1016/j.jcis.2017.11.003.
[33] Ping N, Hans-Jörg B, Bing L, Lu XW, Zhang Y. Phosphate removal from wastewater by model-La (III) zeolite adsorbents. J Environ Sci. 2008;20(6):670–4. doi: 10.1016/S1001-0742(08)62111-7.
[34] Wang Y. Preparation of low-cost fly ash zeolite and its experimental study on synchronous ammonia and phosphorus removal [dissertation]. Changsha: Hunan University; 2011.
[35] García-Lodeiro I, Fernández-Jiménez A, Blanco MT, Palomo A. FTIR study of the sol–gel synthesis of cementitious gels: C–S–H and N–A–S–H. J Sol-Gel Sci Technol. 2008;45:63–72. doi: 10.1007/s10971-007-1643-6.
[36] Karapınar N. Application of natural zeolite for phosphorus and ammonium removal from aqueous solutions. J Hazard Mater. 2009;170(2–3):1186–91. doi: 10.1016/j.jhazmat.2009.05.094.
[37] Hollman GG, Steenbruggen G, Janssen-Jurkovičová. M. A two-step process for the synthesis of zeolites from coal fly ash. Fuel. 1999;78(10):1225–30. doi: 10.1016/S0016-2361(99)00030-7.
[38] Sibrell PL, Kehler T. Phosphorus removal from aquaculture effluents at the northeast fishery center in Lamar, Pennsylvania using iron oxide sorption media. Aquac Eng. 2016;72:45–52. doi: 10.1016/j.aquaeng.2016.04.003.
[39] Liu L, Ma D, Zheng H, Li XJ, Cheng MJ, Bao XH. Synthesis and characterization of microporous carbon nitride. Microporous Mesoporous Mater. 2008;110(2–3):216–22. doi: 10.1016/j.micromeso.2007.06.012.
[40] Liu MW, Wang CZ, Guo JB, Zhang LH. Removal of phosphate from wastewater by lanthanum modified bio-ceramisite. J Environ Chem Eng. 2021;9(5):106123. doi: 10.1016/j.jece.2021.106123.
[41] Han RP, Zhang JJ, Han P, Wang YF, Zhao ZH, Tang MS. Study of equilibrium, kinetic and thermodynamic parameters about methylene blue adsorption onto natural zeolite. Chem Eng J. 2009;145(3):496–504. doi: 10.1016/j.cej.2008.05.003.
[42] Revellame ED, Fortela DL, Sharp W, Hernandez R, Zappi ME. Adsorption kinetic modeling using pseudo-first order and pseudo-second order rate laws: A review. Clean Eng Technol. 2020;1:100032. doi: 10.1016/j.clet.2020.100032.
[43] Malash GF, El-Khaiary MI. Piecewise linear regression: A statistical method for the analysis of experimental adsorption data by the intraparticle-diffusion models. Chem Eng J. 2010;163(3):256–63. doi: 10.1016/j.cej.2010.07.059.
[44] Largitte L, Pasquier R. A review of the kinetics adsorption models and their application to the adsorption of lead by an activated carbon. Chem Eng Res Des. 2016;109:495–504. doi: 10.1016/j.cherd.2016.02.006.
[45] Arris S, Lehocine MB, Meniai AH. Sorption study of chromium sorption from wastewater using cereal by-products. Int J Hydrog Energy. 2016;41(24):10299–310. doi: 10.1016/j.ijhydene.2014.09.147.
[46] Kong XK, Han ZT, Zhang W, Song L, Li H. Synthesis of zeolite-supported microscale zero-valent iron for the removal of Cr6+ and Cd2+ from aqueous solution. J Environ Manage. 2016;169:84–90. doi: 10.1016/j.jenvman.2015.12.022.
[47] Lima EC, Gomes AA, Tran HN. Comparison of the nonlinear and linear forms of the van't Hoff equation for calculation of adsorption thermodynamic parameters (ΔS° and ΔH°). J Mol Liq. 2020;311:113315. doi: 10.1016/j.molliq.2020.113315.